High-contrast top-emitting organic light-emitting devices*

Chen Shu-Fen(陈淑芬), Chen Chun-Yan(陈春燕), Yang Yang(杨 洋), Xie Jun(谢 军), Huang Wei(黄 维)†, Shi Hong-Ying(石弘颖), and Cheng Fan(程 凡)

Key Laboratory for Organic Electronics and Information Displays of Jiangsu Province, Institute of Advanced Materials, Nanjing University of Posts and Telecommunications, Nanjing 210046, *China*

(Received 14 March 2012; revised manuscript received 22 May 2012)

In this paper we report on a high-contrast top-emitting organic light-emitting device utilizing a moderate-reflection contrast-enhancement stack and a high refractive index anti-reflection layer. The contrast-enhancement stack consists of a thin metal anode layer, a dielectric bilayer, and a thick metal underlayer. The resulting device, with the optimized contrast-enhancement stack thicknesses of Ni (30 nm)/MgF_2 (62 nm)/ZnS (16 nm)/Ni (20 nm) and the 25-nm-thick ZnS anti-reflection layer, achieves a luminous reflectance of 4.01% in the visible region and a maximum current efficiency of 0.99 cd/A (at 62.3 mA/cm^2) together with a very stable chromaticity. The contrast ratio reaches 561:1 at an on-state brightness of 1000 cd/m^2 under an ambient illumination of 140 lx. In addition, the anti-reflection layer can also enhance the transmissivity of the cathode and improve light out-coupling by the effective restraint of microcavity effects.

Keywords: top-emitting organic light-emitting device, contrast-enhancement stack, anti-reflection

PACS: 85.60.Jb, 78.60.Fi, 78.66.Qn, 78.40.–q **DOI:** 10.1088/1674-1056/21/10/108506

1. Introduction

Top-emitting organic light-emitting devices (OLEDs)[1,2] are of increasing interest due to their several favourable merits over bottom-emitting ones.[3,4] For example, the aperture ratio of the top-emitting OLED is much higher than that of the bottom-emitting device, since the thin-film transistor can be buried under the bottom anode and the light is extracted from the top cathode in a top-emitting OLED. The high aperture ratio characteristics of a top-emitting OLED make it preferred in the design of an active-matrix OLED, and also provide the possibility of realizing microdisplays of Si substrates. Top-emitting and conventional bottom-emitting OLEDs each are generally composed of a reflective back electrode, a stack of organic functional multilayers, and a (semi-)transparent electrode for light out-coupling. Due to the high reflection of the back electrode, an OLED generally exhibits intensively luminous reflectance, and thereby presents a rather low pixel contrast ratio (PCR) under strong ambient illumination, which is undesirable for many applications.

A variety of approaches to obtaining high-contrast bottom-emitting OLEDs have been proposed, such as bonding circular polarizers,[5] inserting extra layers for optical purposes,[6] using structures of low-reflection cathodes,[6−10] and so on. Until recently, a small number of papers about the improvement of contrast ratio in top-emitting OLEDs have been published, in all of those papers efforts were made to reduce the luminous reflectance (R_L) of the device. Yang *et al.*[11] constructed a top-emitting OLED with a R_L of $\sim 3.9\%$ by utilizing the Mo bottom anode and the anti-reflection coating capping layer on the top cathode. Xie *et al.*[12] demonstrated a top-emitting OLED with a R_L of 13% by employing Au as an anode, copper-phthalocyanine as the hole injection layer, and samarium (Sm) as the cathode. Chen *et al.*[13] obtained a R_L of 23.9% by fabricating a top-emitting OLED with a low reflectance p-type Si bottom anode

*Project supported by the State Key Development Program for Basic Research of China (Grant No. 2009CB930600), the National Natural Science Foundation of China (Grant Nos. 60907047, 61274065, 60977024, 21101095, 20974046, 21003076, 51173081, and 61136003), the Specialized Research Foundation for the Doctoral Program of Higher Education, China (Grant No. 20093223120003), the Natural Science Foundation of Institutions of Higher Education of Jiangsu Province, China (Grant Nos. SJ209003, 09KJB150009, 10KJB510013, and TJ209035), the "Qing Lan" Program of Jiangsu Province, China, and the Program of Nanjing University of Posts and Telecommunications, China (Grant Nos. NY210015, NY211069, and NY210040).

†Corresponding author. E-mail: wei-huang@njupt.edu.cn

© 2012 Chinese Physical Society and IOP Publishing Ltd

and a high transmittance Cs_2CO_3/Ag top cathode.[13]

In the present paper, we introduce a top-emitting OLED with a configuration of Ni/MgF_2/ZnS/Ni/MoO_x (3 nm)/4, 4′, 4″-tris (3-methylphenylphenylamino) (*m*-MTDATA, 45 nm)/4, 4′-bis[N-(1-naphthyl-1-)-N-phenyl-amino]-biphenyl (NPB, 5 nm)/tris(8-hydroxyquinoline) aluminum (Alq_3, 50 nm)/Sm (15 nm)/Ag (10 nm)/ZnS, where the structures of Ni/MgF_2/ZnS/Ni and ZnS are denoted as the moderate-reflection contrast-enhancement stack (CES) and the anti-reflection (AR) layer with optimized thicknesses of Ni (30 nm)/MgF_2 (62 nm)/ZnS (16 nm)/Ni (20 nm) and 25 nm, respectively. The thicknesses of the MgF_2/ZnS bilayer and the AR layer are optimized with a transfer matrix method[14] to minimize the spectral reflectance, $R(\lambda)$, of the device. It achieves an R_L value of 4.01%, corresponding to the contrast ratio reaching 561:1 under an ambient illumination of 140 lx and an on-state brightness of 1000 cd/m^2. It is also desirable to notice that we simply use the optical characteristics of the CES and the AR capping layer outside the active region, which is unlike the previous high-contrast OLED in that it involves inserting an extra layer into the active region of the device.

2. Experimental details

Figure 1 shows the structures of devices involved in this paper. Si coated with a 1600-nm SiO_2 layer is used as the substrate. The organic multilayers in sequence consist of *m*-MTDATA (45 nm) as the hole injection layer, NPB (5 nm) as the hole transport layer, and Alq_3 (50 nm) as the emissive and electron transport layer. Sm (15 nm) with a low work function ($\sim$ 2.7 eV) and low reflectivity in the visible range serves as a semitransparent cathode. A 10-nm-thick Ag film overlays the cathode to guarantee a long lifetime and stable electroluminescence performance. The resulting top-emitting OLED (device A) has the following configuration of Si/SiO_2/Ni (30 nm)/MgF_2 (62 nm)/ZnS (16 nm)/Ni (20 nm)/MoO_x (3 nm)/*m*-MTDATA/NPB/Alq_3/Sm/Ag/ZnS (25 nm), where the structure of Ni (30 nm)/MgF_2 (62 nm)/ZnS (16 nm)/Ni (20 nm) is denoted as the moderate-reflection CES and the 25-nm-thick ZnS as the AR layer. The thicknesses of the Ni/MgF_2/ZnS/Ni CES and the AR layer have been optimized with a transfer matrix method[14] to minimize the spectral reflectance of device. Device B, without the AR layer with respect to device A, is investigated to observe the influence of the AR layer on the reflectance characteristic of the device. For comparison, a control device (Device C)

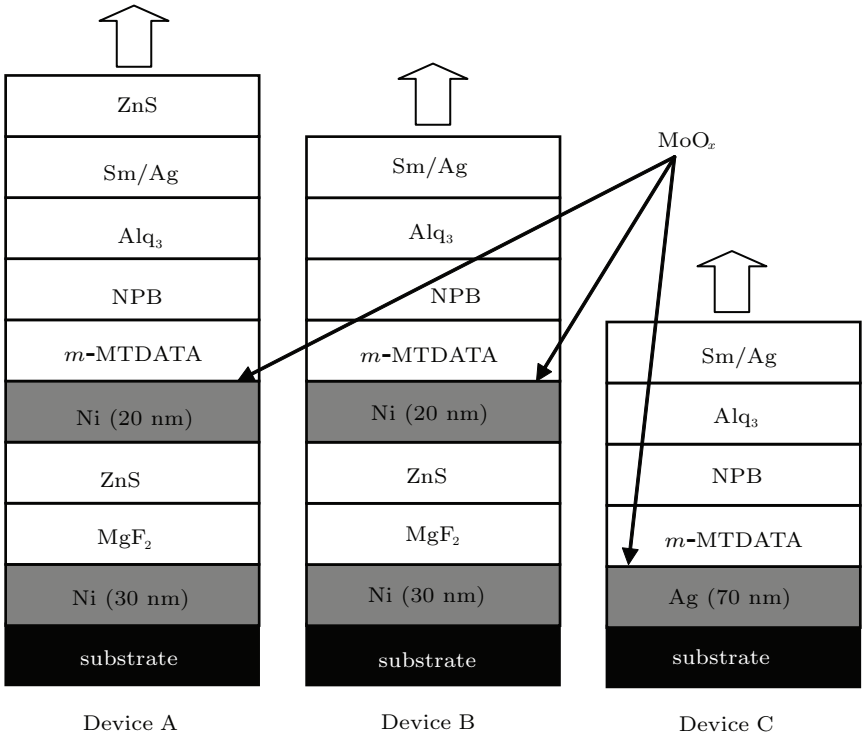


Fig. 1. Schematic structures of devices A, B, and C.

in which the conventional highly-reflective Ag (70 nm) single-layer is used as an anode is also introduced, and its organic multilayers and Sm/Ag cathode structure are the same as those of Device A.

1600-nm-thick SiO_2-covered silicon substrates are cleaned with acetone and ethanol using an ultrasonic bath, rinsed with deionized water, dried in an oven and then transferred into the vacuum chamber. All depositions are in a high vacuum above 5×10^{-4} Pa with a rate of 0.1 nm/s–0.3 nm/s. The electrical and electroluminescent characteristics of the devices are measured with a Keithley 2400 source measurement unit and a Photo-Research PR-655 SpectraScan Colorimeter in room-temperature air. Optical constants of the organic materials are measured with a variable angle spectroscopic ellipsometry. The reflectance and the transmissivity values of the multilayer thin film systems are calculated using the transfer matrix method.

3. Results and discussion

Figure 2 shows the calculated reflectance of the CES structure and the Ag anode. The optimized CES exhibits a moderate reflectivity in the entire visible range of 380 nm–780 nm, which is helpful for reducing the reflectance of the ambient light. From the calculated $R(\lambda)$ values of the three devices in Fig. 3, we find that Device A performs a significantly lower reflectance. A wide low-reflectance band is obtained, with two minima around 430 nm and 630 nm. The difference between the reflectance curves of Devices A and B exhibits that the AR layer is greatly beneficial to the suppression of the reflectance of the entire device structure. Furthermore, we notice that the reflectance of Devices A and B are less dependent on wavelength than that of Device C, which could be attributed to the use of CES. Since the Ag-based anode has a much higher reflectivity, the microcavity effects in Device C are obviously much stronger.

The $R_{\rm L}$ of a device is defined as

$$R_{\rm L} = \int_{\lambda_1}^{\lambda_2} V(\lambda)S(\lambda)R(\lambda)\,{\rm d}\lambda \Big/ \int_{\lambda_1}^{\lambda_2} V(\lambda)S(\lambda)\,{\rm d}\lambda, \quad (1)$$

where λ_1 and λ_2 are 380 nm and 780 nm, respectively, $V(\lambda)$ is the standard photonic curve, and $S(\lambda)$ the spectral power distribution of the light source D65. According to Eq. (1), the calculated $R_{\rm L}$ values for Devices A, B, and C are 4.01%, 25.7%, and 43.4%, respectively.

The PCR of a device is given by

$$\mathrm{PCR} = (L_{\rm on} + R_{\rm L}L_{\rm ambient})/(L_{\rm off} + R_{\rm L}L_{\rm ambient}), \quad (2)$$

where $L_{\rm on}$ and $L_{\rm off}$ are the brightness of a pixel in on- and off-states, respectively, and $L_{\rm ambient}$ is the ambient illumination. Here, $L_{\rm on}$ and $L_{\rm off}$ are set to be 1000 cd/m^2 and 0 cd/m^2, respectively. Figure 4 shows the variations of the calculated PCR of Devices A, B, and C under different ambient illuminations. As shown in Fig. 4, the PCRs of Device A are drastically larger than those of Devices B and C. For instance, the PCR values of Devices A, B, and C are 561:1, 87:1, and 52:1 under the ambient illumination of 140 lx, respectively. And even under a high ambient illumination of 10000 lx, the PCR value in Device A is over 10 times higher than that in Device C.

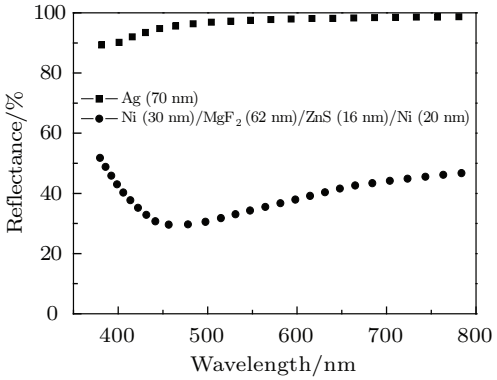


Fig. 2. Calculated reflectance of the Ag anode and the CES structure.

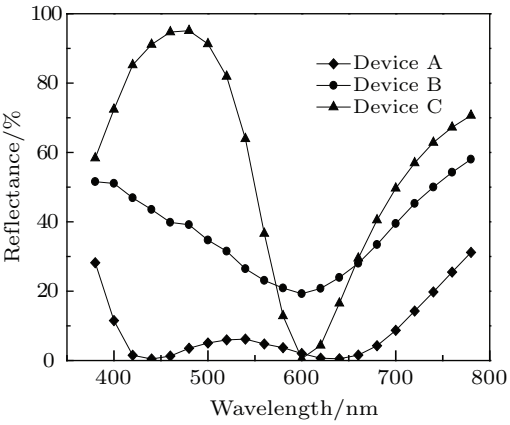


Fig. 3. Calculated reflection spectra for Devices A, B, and C.

Considering the fact that the optical interference in a device is strongly dependent on the incident angle, the reflection characteristics of the resulting device against different incident angles are discussed here. The calculated reflectance spectra of Device A at viewing angles of 0° (normal to the electrode surface), 30°,

and 60° are displayed in Fig. 5, which indicate that the reflectance of our resulting device is weakly incident angle-dependent, and even at 60° the value is still quite admirable.

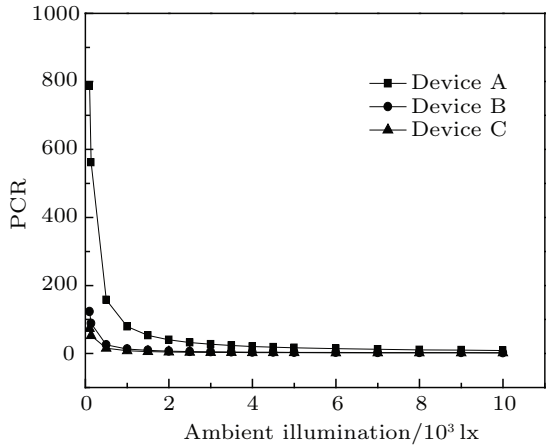


Fig. 4. Calculated contrast ratios of Devices A, B, and C.

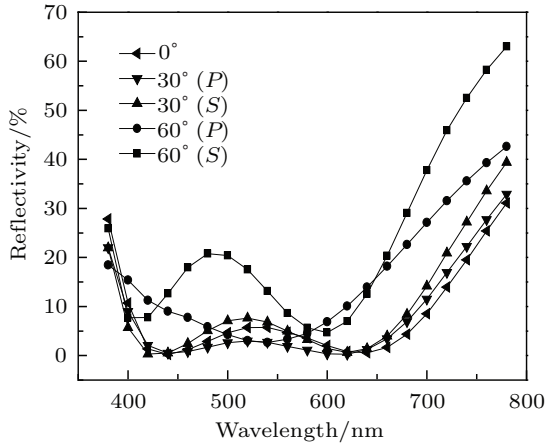


Fig. 5. Calculated reflectance spectra of Device A at viewing angles of 0°, 30°, and 60°.

It has been reported that the out-coupling of emitted light in a top-emitting OLED can be improved by capping a dielectric layer with a proper thickness on the top semitransparent cathode.[15] This inspires us to analyse the influence of the 25-nm-thick ZnS layer on the efficiency of light out-coupling in the resulting device. Assuming that the carrier recombination and light generation take place in the Alq_3 layer and near the Alq_3/NPB interface, light emitted in a direction toward the cathode needs to pass through a stack of Alq_3, Sm, Ag, and ZnS before going into air. By using the transfer matrix method, the transmittivities of The multilayer systems Alq_3/Sm/Ag/ZnS (a), and Alq_3/Sm/Ag (b) are calculated. As shown in Fig. 6, the transmittivity is enhanced from ∼42% to ∼71% at a wavelength of around 550 nm due to the introduction of the ZnS layer, which effectively restrains the influence of microcavity effect on the emission colour and improves the out-coupling light intensity.

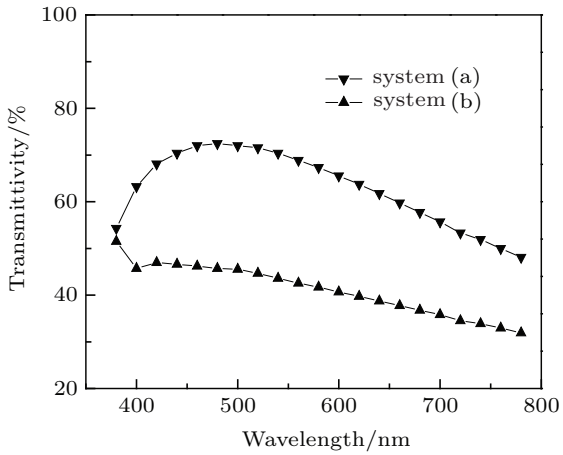


Fig. 6. Calculated transmission spectra of two mutilayer systems: (a) Alq_3 (50 nm)/Sm (15 nm)/Ag (10 nm)/ZnS (25 nm) and (b) Alq_3 (50 nm)/Sm (15 nm)/Ag (10 nm) at the normal angle.

Figure 7(a) shows the current density–voltage (J–V) characteristics of Devices A, B, and C. We find that the Ag anode-based Device C exhibits a better performance than Devices A and B, which can be explained by the fact that the conductivity of Ag is much higher than that of Ni although the work function of Ag (∼ 4.6 eV) is lower than that of Ni (∼ 5.1 eV). Figure 7(b) exhibits that the brightness–current density (B–J) characteristics of Device C are the best among the three devices, which can be attributed to the high reflectivity and the low resistance of the Ag anode, while the B–J performances of Devices A and B are affected to some extent by morphological deterioration of device films due to the introduction of CES under the OLED. Device A shows a higher brightness value than Device B under the same current density, which proves the AR layer can enhance the out-coupling of emitted light. The maximum current efficiencies of Devices A, B, and C are 0.99 (at 62.3 mA/cm^2), 0.63 (at 39.5 mA/cm^2), and 0.96 (at 57.8 mA/cm^2) cd/A, respectively. Device A also shows that it has the most stable electroluminiscent spectrum characteristics with respect to observation angle among the three devices as shown in Fig. 8, with a Commission International de L'Eclairage (CIE) coordinates change of only (0.0134, 0.0087) during a large viewing angle change of 0° to 75° though its EL peak, and the full width at half maximum (FWHM) shows an obvious change.

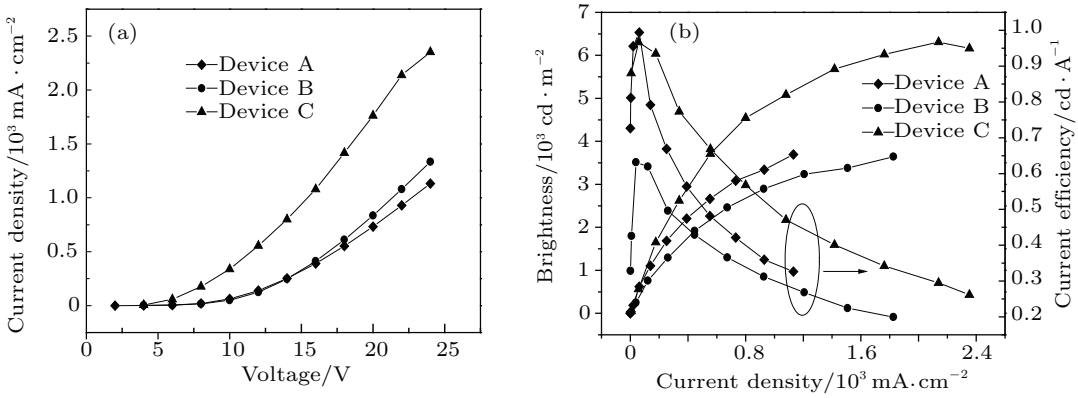


Fig. 7. (a) J–V and (b) B–J characteristics of Devices A, B, and C.

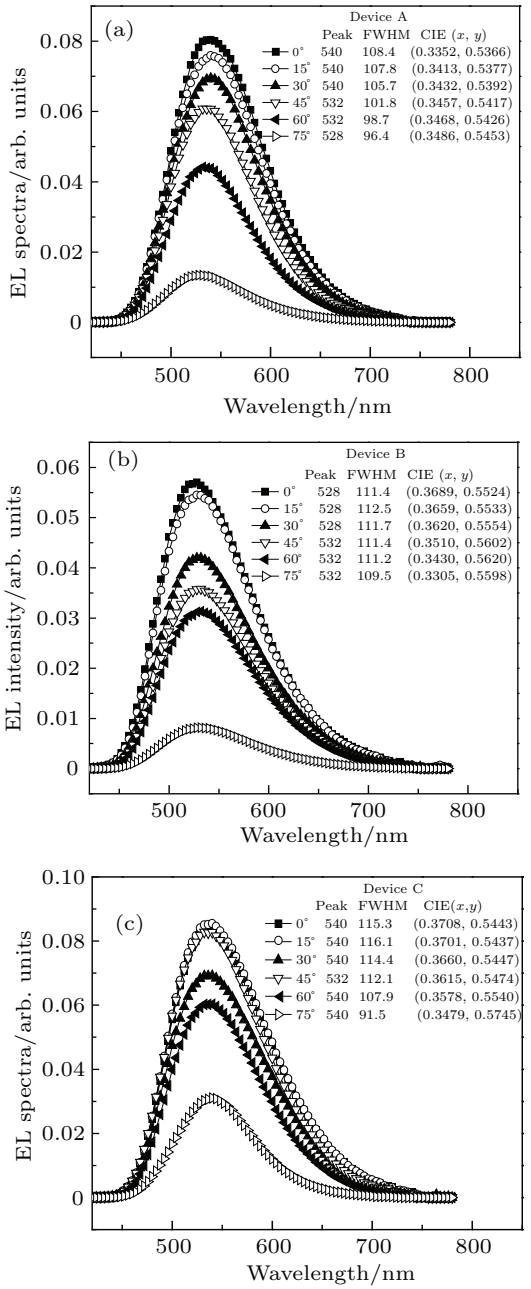


Fig. 8. Electroluminiscent spectra with different observation angles for Devices A, B, and C.

4. Conclusions

In this paper, we demonstrate a high-contrast configuration of a top-emitting OLED with a moderate-reflection contrast-enhancement stack of Ni (30 nm)/MgF_2 (62 nm)/ZnS (16 nm)/Ni (20 nm) and an anti-reflection layer of 25-nm-thick ZnS layer capping on the cathode. A maximum current efficiency of 0.99 cd/A is achieved at 62.3 mA/cm^2 and an extremely stable chromaticity is obtained with a CIE coordinates change of only (0.0134, 0.0087) during a large viewing angle change of 0°–75°. At a pixel brightness of 1000 cd/m^2, a contrast ratio of 561:1 is obtained by our resulting device under an ambient illumination of 140 lx, which is much higher than the 52:1 of the conventional device with an Ag anode. We also find that the utilization of CES causes the device performance to decrease due to morphological deterioration of the device film and the 25-nm-thick ZnS layer is beneficial to the improvement of the light outcoupling from the device due to the effective restraint of microcavity effects.

References

[1] Chen S F, Deng L L, Xie J, Peng L, Xie L H, Fan Q L and Huang W 2010 *Adv. Mater.* **22** 5227
[2] Cao J, Jiang X Y and Zhang Z L 2007 *Acta Phys. Sin.* **56** 3493 (in Chinese)
[3] Nie H, Zhang B and Tang X Z 2007 *Chin. Phys.* **16** 730
[4] Yang Y, Chen S F, Xie J, Chen C Y, Shao M, Guo X and Huang W 2011 *Acta Phys. Sin.* **60** 047809 (in Chinese)
[5] Pucilowski J, Schuman R and Velasquez J 1974 *Appl. Opt.* **13** 2248
[6] Hung L S and Madathil J 2001 *Adv. Mater.* **13** 1787
[7] Krasnov A N 2002 *Appl. Phys. Lett.* **80** 3853
[8] Xie Z Y and Hung L S 2004 *Appl. Phys. Lett.* **84** 1207
[9] Feng X D, Khangura R and Lu Z H 2004 *Appl. Phys. Lett.* **85** 497

[10] Wong F L, Fung M K, Jiang X, Lee C S and Lee S T 2004 *Thin Solid Films* **446** 143

[11] Yang C J, Lin C L, Wu C C, Yeh Y H, Cheng C C, Kuo Y H and Chen T H 2005 *Appl. Phys. Lett.* **87** 143507

[12] Xie W F, Sun H Y, Law C W, Lee C S and Liu S Y 2006 *Appl. Phys.* A: *Mater. Sci. & Process.* **85** 95

[13] Chen S M, Yuan Y B, Lian J R and Zhou X 2007 *Opt. Express* **15** 14644

[14] Dobrowolski J A, Sullivan B T and Bajcar R C 1992 *Appl. Opt.* **31** 5988

[15] Chen S F, Xie W F, Huang W and Liu S Y 2008 *Opt. Express* **16** 8868